Catal Lett (2011) 141:235–241
DOI 10.1007/s10562-010-0462-5

$Rh_{1-x}Pd_x$ Nanoparticle Composition Dependence in CO Oxidation by NO

James Russell Renzas · Wenyu Huang · Yawen Zhang · Michael E. Grass · Gabor A. Somorjai

Received: 19 August 2010 / Accepted: 2 October 2010 / Published online: 13 November 2010

Abstract Bimetallic 15 nm Pd-core Rh-shell $Rh_{1-x}Pd_x$ nanoparticle catalysts have been synthesized and studied in CO oxidation by NO. The catalysts exhibited composition-dependent activity enhancement (synergy) in CO oxidation in high NO pressures. The observed synergetic effect is attributed to the favorable adsorption of CO on Pd in NO-rich conditions. The Pd-rich bimetallic catalysts deactivated after many hours of oxidation of CO by NO. After catalyst deactivation, product formation was proportional to the Rh molar fraction within the bimetallic nanoparticles. The deactivated catalysts were regenerated by heating the sample in UHV. This regeneration suggests that the deactivation was caused by the adsorption of nitrogen atoms on Pd sites.

Keywords Nanoparticle · Bimetallic · Catalysis · Composition dependence · CO Oxidation · NO

J. R. Renzas · W. Huang · G. A. Somorjai (✉)
Department of Chemistry, University of California, Berkeley, CA 94720, USA
e-mail: somorjai@berkeley.edu

J. R. Renzas · W. Huang
Chemical Sciences Division, Lawrence Berkeley National Laboratory, Berkeley, CA 94720, USA

Y. Zhang · G. A. Somorjai
Materials Science Division, Lawrence Berkeley National Laboratory, Berkeley, CA 94720, USA

Y. Zhang
College of Chemistry and Molecular Engineering, State Key Lab of Rare Earth Materials Chemistry and Applications and PKU-HKU Joint Lab in Rare Earth Materials and Bioinorganic Chemistry, Peking University, Beijing 100871, China

M. E. Grass
Advanced Light Source, Lawrence Berkeley National Laboratory, Berkeley, CA 94720, USA

M. E. Grass
Department of Applied Physics, Hanyang University, Ansan 426-791, Korea

1 Introduction

Since the introduction of the three-way catalytic convertor in the 1970s for NO_x reduction and the oxidation of carbon monoxide from automobile exhaust, there have been intensive efforts to understand the fundamental mechanisms underlying these catalytic systems [1]. Despite these efforts, however, attempts to find an appropriate catalyst with high activity for NO_x removal have been met with limited success because of catalyst poisoning from strongly-bound oxygen adsorbates left on the surface from NO dissociation [2]. Rhodium is acknowledged to be the best catalyst for this reaction, with intense efforts devoted to understanding its behavior [3–13]. However, in recent years much research has also been aimed at understanding the role of Pd in the reaction [1–3, 14–19] because of the relatively high cost of rhodium catalysts, palladium's improved resistance to sintering, and because new improvements in gasoline purification have helped reduce the significance of previous problems with Pd site poisoning by sulfur and lead [15]. Pd has been found to have lower activity than Rh for the reaction of NO with CO [16] and has also been shown to suffer from deactivation [14]. The origin of this deactivation has not been definitively identified.

Current developments in the synthesis of structured bimetallic nanoparticle systems have also enabled the study of unique new catalyst systems that were not possible in the past [20]. These new systems can sometimes improve upon

the catalytic performance of previous monometallic systems [21–25]. It has become apparent that these new catalyst systems may provide pathways to increase reactivity and decrease deactivation under the right conditions. The use of a combination of Rh and Pd has been studied for the oxidation of CO by O [22, 1, 25–27], but there has been limited progress on the study of the oxidation of CO by NO [28, 29]. Recently, this system was shown to be of particular interest in ambient pressure X-ray photoelectron spectroscopy (APXPS) experiments, where the X-ray probe depth on the sample can be controlled by varying the energy of the incident X-ray beam from a synchrotron source. With the APXPS technique, we found that the surface of the as-synthesized $Rh_{0.5}Pd_{0.5}$ is Rh-rich, with the atomic fraction of Rh comprising 93% of total surface atoms. We also demonstrated surface-segregation behavior for 15 nm Pd core-Rh shell nanoparticles of different composition ($Rh_{0.2}Pd_{0.8}$, $Rh_{0.5}Pd_{0.5}$, and $Rh_{0.8}Pd_{0.2}$) in the catalytic condition of CO oxidation by NO. We found Pd segregated to the surface of the RhPd nanoparticles at 300 °C under 100 mTorr NO and 100 mTorr of CO, while Rh segregated to the surface of the RhPd nanoparticles at the same temperature under 100 mTorr NO [20, 30]. This work established the surface state of the system in reaction conditions, but did not include kinetic studies. In the current report, we studied the catalytic properties of the same $Rh_{1-x}Pd_x$ nanocrystals studied by APXPS for the oxidation of CO by NO. We also proposed a model to explain the complex catalytic behavior of the $Rh_{1-x}Pd_x$ nanocrystals. These kinetic studies are necessary in order to correlate the surface condition of the core–shell nanoparticle structures with real catalytic behavior. The understanding of the kinetic behavior of these core–shell Rh-Pd nanoparticle catalysts in the oxidation of CO by NO is important for the understanding both of the reaction itself, but also of the behavior of complex core–shell nanoparticle systems in general.

2 Experimental Details

The synthesis and characterization of the $Rh_{1-x}Pd_x$ nanoparticles have been reported previously [31]. In brief, to synthesize 15 nm $Rh_{1-x}Pd_x$ of a given composition, [$(1 - x) \cdot$ 0.1 mmol] rhodium(III) acetylacetonate, ($x \cdot 0.1$ mmol) palladium(II) acetylacetonate, and 1 mmol poly(vinylpyrrolidone) (PVP) (monomer concentration) were added to 20 mL of 1,4 butanediol in a 50 mL three-necked flask. A magnetic stirring rod continuously stirred the solution during synthesis. The solution was heated from room temperature to 50 °C and evacuated at 50 °C for 20 min to remove water and oxygen. The solution was then placed under Ar and heated to 220 °C at 10 °C min^{-1}. The synthesis was complete after 1.5 h at 220 °C. After cooling to room temperature, an excess of acetone was added to the solution to form a suspension. The suspension was separated by centrifugation at 4200 rpm for 6 min and the supernatant was discarded. The remaining product was rinsed with acetone once and then re-dispersed in ethanol. With the above method, we synthesized RhPd nanocrystals with three compositions: $Rh_{0.2}Pd_{0.8}$, $Rh_{0.5}Pd_{0.5}$, and $Rh_{0.8}Pd_{0.2}$ No specific procedure was taken to control the shape of the nanoparticle. The as-synthesized RhPd nanocrystals have an Rh-rich surface measured by APXPS [20, 30].

Monometallic nanoparticles of the same size and shape were synthesized similarly, except that the Pd monometallic nanoparticles were only kept at 220 °C for 0.5 h and the Rh monometallic nanoparticles were synthesized using 0.2 mmol of $Rh(acac)_3$, evacuated at 140 °C, and reacted at 205 °C for 2 h.

All catalytic samples were prepared using the Langmuir–Blodgett (LB) method [31]. Prior to deposition, the nanoparticles were washed by repeatedly dispersing in ethanol and precipitating in hexane (early wash cycles) or dispersing in chloroform and precipitating in hexane (later wash cycles) to remove impurities and excess PVP. Monolayers of nanoparticles were formed by placing drops of nanoparticle solution (dispersed in chloroform) onto the surface of water in a LB trough. The surface was compressed to a surface pressure of 11 mN/m and *p*-type (100) Si wafers (1 cm^2 pieces) were lifted up from below the surface of the water such that the resulting films had nanoparticle surface coverage of 15–30%.

The CO oxidation by NO reactions were performed in a reaction chamber which has also been described previously [13]. This chamber consisted of a 1 L reaction cell connected to a gas chromatograph (GC) in batch mode with a mechanical recirculation pump located between the cell and GC. Temperature was controlled with a ceramic button heater (Momentiv) and measured with a type-k thermocouple placed on the sample surface. The reaction was run from 220 to 260 °C on the $Rh_{1-x}Pd_x$ nanocrystals in batch mode in 8 Torr CO, 8–120 Torr NO, and 632–744 Torr He, such that the total pressure was always 760 Torr. This temperature range was chosen to ensure adequate turnover for the nanocrystal samples without significant particle aggregation on the surface of the Si wafer. Turnover frequency was calculated independently for the formation of each product, CO_2, N_2, and N_2O.

3 Results

CO oxidation by NO was carried out in 8 Torr CO, 8 Torr NO, and 744 Torr He carrier gas. The nanocrystals were stable in reaction at 260 °C, as shown by SEM in Fig. 1, but underwent significant aggregation at 275 °C.

Consequently, the reaction temperature was kept at 260 °C and below for all experiments presented here.

Turnover frequencies versus Pd molar fraction at 230, 240, 250, and 260 °C for the formation of CO_2, N_2, and N_2O have similar trends and the data at 230 and 260 °C are presented in Fig. 2a–c, respectively. Turnover frequency decreased with increased Pd molar fraction and increased with temperature for all products. At high temperature, the bimetallic nanocrystals underperformed relative to the theoretical activity of a linear combination of pure Rh and pure Pd nanocrystals, based on the performance of the Rh and Pd nanocrystals studied here. Selectivity towards N_2O, defined as $S = TOF_{N_2O}/(TOF_{N_2O} + TOF_{N_2}) \times 100\%$, is presented in Fig. 2d and is found to decrease with increased molar fraction of Pd in this temperature range.

Experimentally measured activation energies for the formation of the CO_2, N_2O, and N_2 products in 8 Torr NO, 8 Torr CO, and 744 Torr He are presented in Fig. 3. Activation energy was found to decrease with increased Pd molar fraction for all products. No activation energies are presented for the 100% Pd nanocrystals due to extremely low turnover frequencies for all products in these reaction conditions. These results compare relatively well to previous studies on Rh and Pd nanoparticle catalysts, such as studies by Granger et al., who found higher turnover rates and activation energies on Rh/Al_2O_3 catalysts as compared to Pd/Al_2O_3 catalysts [16]. No synergism was observed in these conditions with the $Rh_{1-x}Pd_x$ nanocrystals.

The reaction between NO and CO was also carried out under excess NO, in 80 Torr NO, 8 Torr CO, and 672 Torr He and a stepped temperature ramp from 230 to 260 °C in 10 °C increments with 3 h at each step. Figure 4a demonstrates that at 230 °C, prior to deactivation, the Pd-rich catalysts were more active for CO_2 production than the Rh-rich catalysts. Before deactivation, the $Rh_{1-x}Pd_x$ nanoparticles also become more active for CO oxidation as the NO to CO ratio is increased. For example, the $Rh_{0.2}Pd_{0.8}$ catalysts produced eleven times more CO_2 in 80 Torr NO than in 8 Torr NO at 230 °C. Interestingly, N_2O and N_2 production were not significantly enhanced.

After 3 h at both 230 and 240 °C, the Pd-rich nanoparticles deactivated. The deactivation was relatively abrupt and exhibited a strong dependence on the composition of the bimetallic catalyst. In general, Pd-rich nanoparticles deactivated more than Rh-rich ones. The catalyst activity after deactivation was typically similar to a linear combination of Rh and Pd monometallic catalyst for all three products. We also found that heating the sample to 150 °C in UHV for 1 h restores the activity of the catalyst. Decreasing the temperature in reaction, however, did not restore the pre-deactivation activity. A reaction mechanism for the deactivation and reactivation of the catalysts is proposed in the Sect. 4.

The role of NO pressure in the activity of the Pd-rich nanocatalysts was further investigated using a stepped temperature ramp from 220 to 250 °C in 10 °C increments with 3 h at each step, a fixed CO pressure of 8 Torr, and NO pressures ranging from 20 to 120 Torr. The turnover frequency of CO_2 is presented in Fig. 4b for each condition. Interestingly, at 220 °C, prior to deactivation, the turnover frequency was strongly dependent on P_{NO}, whereas the turnover frequency was virtually independent of P_{NO} at 250 °C, after deactivation. N_2O and N_2 production followed similar trends to the 80 Torr NO condition discussed above. Again, heating the sample to 150 °C in UHV for 1 h was found to restore the catalyst activity.

4 Discussion

In their monometallic state, these two metals have very different catalytic behavior in CO oxidation by NO. The Rh nanoparticles were very active, had a moderate decrease in activity at elevated pressures of NO, and did not undergo significant deactivation. These results are consistent with previous studies on Rh catalysts in this reaction, which found that supported Rh nanoparticles show decreased activity with increased NO pressure at 538 K [32] and that Rh shows very little deactivation for this reaction [33]. The Pd nanoparticles, however, were significantly less active in all conditions and deactivated at elevated pressure of NO. These results, again, are consistent with previous studies on Pd catalysts in this reaction, which found that the activity of Pd is positive order in NO [34], and the deactivation of Pd is quite significant [14, 15].

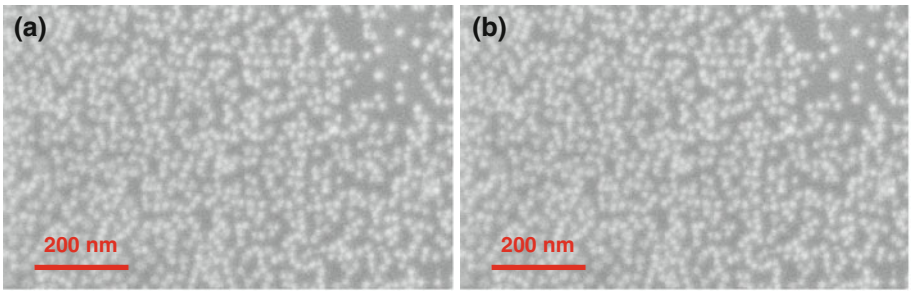

Fig. 1 SEM of $Rh_{0.5}Pd_{0.5}$. **a** Before and **b** after reaction in 8 Torr NO, 8 Torr CO, 744 Torr He at 260 °C. No significant morphological change is observed after reaction at this temperature

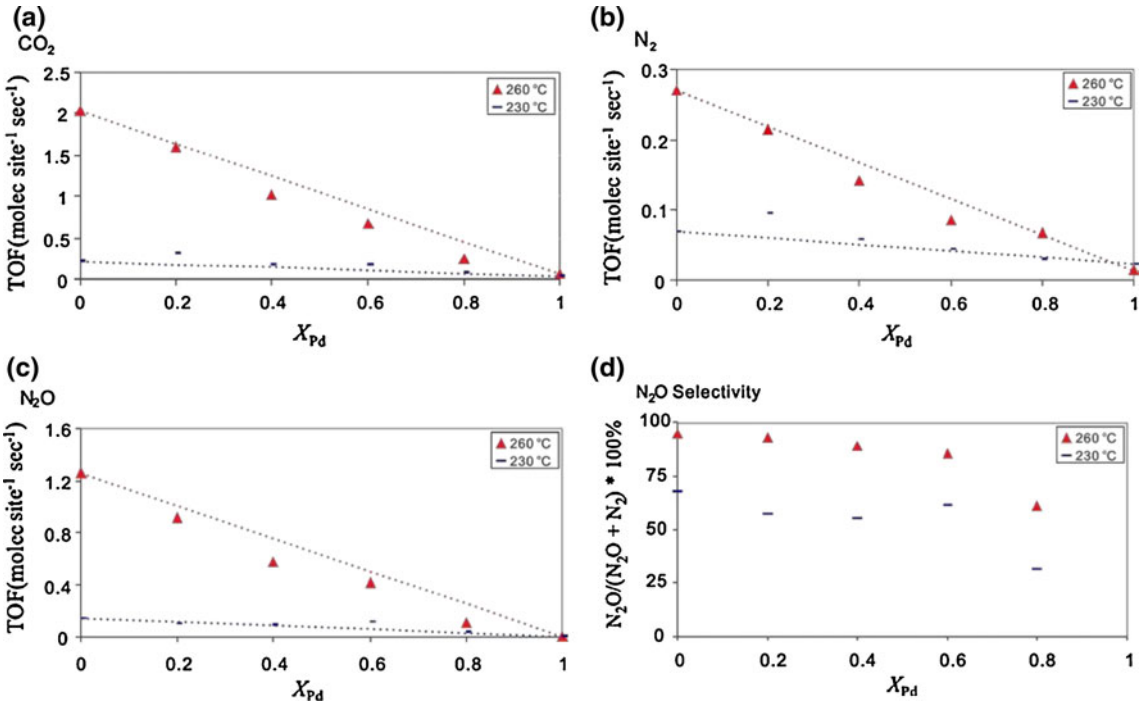

Fig. 2 Turnover frequency for formation of **a** CO_2, **b** N_2, and **c** N_2O products and selectivity towards N_2O as a function of Pd molar fraction for $Rh_{1-x}Pd_x$ nanocrystals in 8 Torr NO, 8 Torr CO, 744 Torr He at 230 and 260 °C. No synergetic effects were observed in these reaction conditions. *Dash lines* in **a**–**c** represent the TOF for physical mixtures of Pd and Rh nanocrystals

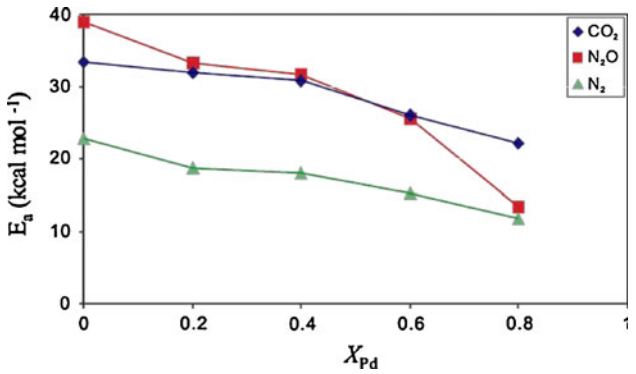

Fig. 3 Activation energy for formation of CO_2, N_2O, and N_2 products as a function of Pd molar fraction for $Rh_{1-x}Pd_x$ nanocrystals in 8 Torr NO, 8 Torr CO, 744 Torr He from 230 to 260 °C. The low activity of the pure Pd nanocrystals made determination of an accurate activation energy difficult for those samples

The behavior of the bimetallic catalysts in the $P_{NO} = P_{CO}$ condition is fairly similar to the behavior of a linear combination of monometallic catalyst. No synergetic effect is observed and the catalyst activity is slightly worse than an equivalent linear combination of monometallic catalyst, perhaps due to Pd-enrichment in the surface layers in this condition, which is the most reducing condition in this study. This observation is consistent with APXPS data, which showed that Pd is slightly enriched on the surface and Rh is almost completely metallic when $P_{NO} = P_{CO}$ at 300 °C [20]. The metallic nature of the Rh surface indicates that NO is not rapidly dissociated by Rh in these conditions.

In the $P_{NO} > P_{CO}$ condition, however, the bimetallic catalysts showed markedly different behavior. The observed synergy and subsequent deactivation indicate that the Rh and Pd components of the catalyst are interacting in important ways. The model we propose is that prior to deactivation, isolated Pd atoms serve as preferential adsorption sites for CO, while high pressure of NO favors dissociative adsorption of NO on Rh. The CO_2 formation step in the reaction occurs when oxygen adsorbates spillover from Rh sites to Pd sites and react with CO molecules adsorbed on Pd. N_2O and N_2 formation were not significantly enhanced in this regime, which indicates that the presence of Pd in these catalysts does not play a significant role for the formation of those products. Our observations suggest that, for these bimetallic catalysts, Pd effectively acts as a promoter, facilitating adsorption of CO while Rh dissociates NO.

This model is also well-supported by existing literature. It is known that the efficient dissociative adsorption of NO on monometallic Rh is self-inhibited at high NO coverages, which limits the coverage of CO on the surface and thus the reaction rate [11]. It is also known that NO adsorption is relatively unfavorable on Pd, which renders the Pd sites available for the adsorption of CO even in NO-rich

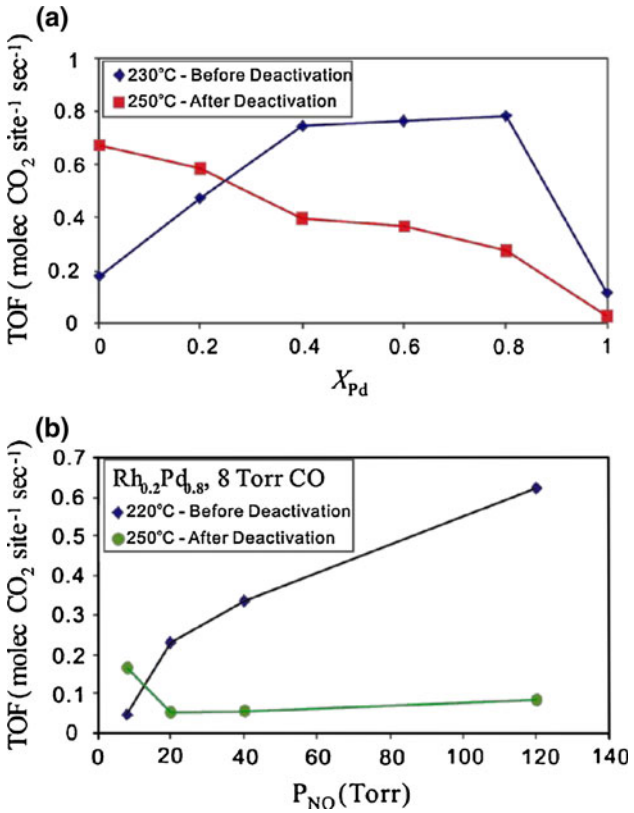

Fig. 4 **a** TOF of CO_2 as a function of Pd molar fraction for $Rh_{1-x}Pd_x$ nanocrystals at 230 °C (before deactivation) and 250 °C (after deactivation) in 80 Torr NO, 8 Torr CO, and 672 Torr He. **b** TOF of CO_2 as a function of NO pressure for $Rh_{0.2}Pd_{0.8}$ nanocrystals in 8 Torr CO and a total pressure of 760 Torr equalized with He. A significant synergetic effect was observed in the catalytic activity of Pd-rich $Rh_{1-x}Pd_x$ bimetallic nanocrystals at elevated NO pressures prior to deactivation

conditions [35]. Additionally, infrared spectroscopy on Rh/Al_2O_3 and Pd/Al_2O_3 by Granger et al., found that the reaction rate is highest when the coverage of NO is much greater than CO but not high enough to be inhibiting, and that CO adsorbs preferentially on 10 wt% Pd/Al_2O_3, which has a crystallite size comparable to the nanoparticle size in the present study [16]. Our previous APXPS experiments also showed that Rh atoms segregate to the surface and oxidize in NO, even after pre-exposure of the bimetallic nanoparticles to CO [20]. Although it is possible for NO to adsorb molecularly on Rh, the strong Rh oxidation observed in APXPS implies that a significant portion of NO is dissociatively adsorbed. Together, this data supports the notion that CO adsorption on Pd sites in the bimetallic catalyst, in combination with oxygen spillover from NO molecules dissociatively adsorbed on Rh sites in high pressure of NO, is likely to increase the CO_2 production of the catalyst prior to deactivation.

The cause of deactivation on the Pd-rich bimetallic catalysts is also of considerable interest. In this case, the most probable explanation is that Pd is eventually poisoned by spillover of N atoms from Rh. This model is supported by the work of Vesecky, Rainer, and Goodman, who used Temperature Programmed Desorption (TPD) to show that high surface area Pd catalysts and Pd (100) single crystals are poisoned by stable adsorbed nitrogen atoms, and that free surface oxygen is removed so quickly by CO to form CO_2 that it is unlikely to play a role in the catalyst deactivation [36]. This explanation for deactivation seems more likely than previously suggested mechanisms, such as reaction inhibition by carbon deposition on the surface [14] or self-inhibited NO adsorption on the Rh surface [11] because deactivation was not observed on the pure-Rh catalyst despite identical reaction conditions, and because the sample activity was closely correlated with the Rh molar fraction after deactivation. The importance of nitrogen in this deactivation is further supported by the observation that N_2O and N_2 production were not significantly enhanced prior to catalyst deactivation. This indicates that adsorbed nitrogen is not effectively removed from the catalyst surface.

In this scenario for deactivation, once Pd is poisoned the catalytic activity is dominated by the availability of Rh sites on the catalyst surface because Pd can no longer act as a promoter. Figure 4a supports this notion, as the catalyst activity increased with Rh molar fraction in a roughly linear fashion at 250 °C, after deactivation. If this is indeed the case, the 150 °C UHV heating step may restore activity by removing adsorbed nitrogen from the catalyst surface.

There are several outstanding considerations which must be taken into consideration in examining the simple synergetic and deactivation models suggested here. First, much of our model is predicated on our previous results in APXPS, but there is a pressure gap between that study, which was carried out at tenths of a Torr [20], and this study, which was carried out in tens of Torr of reaction gases mixed with He for a total pressure of one atmosphere. Since the entropic contribution of the Gibbs Free Energy increases as $kT \cdot \log P$, this pressure gap leads to an energy difference which ranges from 0.09 eV at 27 °C and 0.18 eV at 300 °C. Although this is a dramatic improvement from the 0.28 and 0.54 eV energy differences at 27 and 300 °C between reaction at atmosphere and analysis at 10^{-8} Torr, as required for traditional XPS or Auger analysis, further improvement is necessary. We are currently building a reactor capable of measuring kinetics in conditions identical to those used in APXPS which will enable even more precise study of the role of surface segregation and oxidation in catalysis.

In summary, NO reduction by CO is known to be an exceedingly complex reaction dependent on many subtle factors, such as stable islands of adsorbed N on Rh [19, 36–38] and the oxidation state of the metals [3, 39, 40].

Although the model proposed here is consistent with our kinetic data, further studies are needed to fully understand the initial catalyst behavior and subsequent deactivation of bimetallic Pd-core Rh-shell $Rh_{1-x}Pd_x$ nanocrystals.

5 Conclusions

15 nm $Rh_{1-x}Pd_x$ Pd-core Rh-shell nanocrystals were synthesized, characterized, and studied in the catalytic oxidation of CO by NO. A model based on available literature was proposed to help explain the observed catalytic behavior. Although no synergy was observed in the NO/CO reaction when $P_{NO} = P_{CO} = 8$ Torr, the Pd-rich bimetallic catalysts were very active at 8 Torr CO and 80 Torr NO prior to undergoing deactivation. Pd enhances the reaction by ensuring adequate adsorption of CO in the high NO coverage regime. Pd is eventually poisoned by adsorbed N and reactivity is dominated by the availability of Rh surface sites. These results demonstrate unique and desirable synergetic behavior in bimetallic core–shell catalysts and will hopefully lead to greater understanding of the many complex factors governing reactivity in these systems.

Acknowledgements This work was supported by the Director, Office of Science, Office of Basic Energy Sciences, of the U.S. Department of Energy under Contract No. DE-AC02-05CH11231. Y.W.Z. gratefully acknowledges the financial aid of Huaxin Distinguished Scholar Award from Peking University Education Foundation of China.

References

1. Rainer DR, Vesecky SM, Koranne M, Oh WS, Goodman DW (1997) The CO + NO reaction over Pd: a combined study using single-crystal, planar-model-supported, and high-surface-area Pd/Al_2O_3 catalysts. J Catal 167(1):234–241
2. Pisanu AM, Gigola CE (1999) NO decomposition and NO reduction by CO over Pd/ [alpha]-Al_2O_3. Appl Catal B: Environ 20(3):179–189
3. Almusaiteer K, Chuang SSC (1999) Dynamic behavior of adsorbed NO and CO under transient conditions on Pd/Al_2O_3. J Catal 184(1):189–201
4. Araya P, Gracia F, Cortes J, Wolf EE (2002) FTIR study of the reduction reaction of NO by CO over Rh/SiO_2 catalysts with different crystallite size. Appl Catal B-Environ 38(2):77–90
5. Avalos LA, Bustos V, Unac R, Zaera F, Zgrablich G (2005) Toward a realistic model for the kinetics of the NO plus CO reaction on rhodium surfaces. J Mole Catal A-Chem 228(1–2): 89–95
6. Bustos V, Gopinath CS, Unac R, Zaera F, Zgrablich G (2001) Lattice-gas study of the kinetics of catalytic conversion of NO–CO mixtures on rhodium surfaces. J Chem Phys 114(24): 10927–10931
7. Herman GS, Peden CHF, Schmieg SJ, Belton DN (1999) A comparison of the NO–CO reaction over Rh(100), Rh(110) and Rh(111). Catal Lett 62(2–4):131–138
8. Hopstaken MJP (2000) Elementary reaction kinetics and lateral interactions in the catalytic reaction between NO and CO on rhodium surfaces. Eindhoven University of Technology, Eindhoven, The Netherlands
9. Hopstaken MJP, Niemantsverdriet JW (2000) In reaction between NO and CO on rhodium (100): how lateral interactions lead to auto-accelerating kinetics. J Vac Sci Technol 18:1503–1508
10. Peden CHF, Belton DN, Schmieg SJ (1995) Structure sensitive selectivity of the NO–CO reaction over Rh(110) and Rh(111). J Catal 155(2):204–218
11. Permana H, Ng KYS, Peden CHF, Schmieg SJ, Belton DN (1995) Effect of no pressure on the reaction of no and co over Rh(111). J Phys Chem 99(44):16344–16350
12. Permana H, Ng KYS, Peden CHF, Schmieg SJ, Lambert DK, Belton DN (1996) Adsorbed species and reaction rates for NO–CO over Rh(111). J Catal 164(1):194–206
13. Renzas JR, Zhang Y, Huang WY, Somorjai GA (2009) Rhodium nanoparticle shape dependence in the reduction of NO by CO. Catal Lett 132:317–322
14. Cortes J, Valencia E, Aguila G, Orellana E, Araya P (2008) Time decay of the activity of the reduction reaction of NO by CO on a Pd/Al_2O_3 catalyst. Catal Lett 126(1–2):63–71
15. Cortes J, Valencia E, Herrera J, Araya P (2007) Mechanism and kinetics parameters of the reduction reaction of NO by CO on Pd/Al_2O_3 catalyst. J Phys Chem C 111(19):7063–7070
16. Granger P, Dhainaut F, Pietrzik S, Malfoy P, Mamede AS, Leclercq L, Leclercq G (2006) An overview: comparative kinetic behaviour of Pt, Rh and Pd in the NO + CO and NO + H_2 reactions. Top Catal 39(1–2):65–76
17. Holles JH, Davis RJ, Murray TM, Howe JM (2000) Effects of Pd particle size and ceria loading on NO reduction with CO. J Catal 195(1):193–206
18. Kobal I, Kimura K, Ohno Y, Matsushima T (2000) Angular and velocity distributions of desorbing molecules in steady-state NO plus CO reaction on Pd(110). Surf Sci 445(2–3):472–479
19. Vesecky SM, Chen PJ, Xu XP, Goodman DW (1995) Evidence for structure sensitivity in the high-pressure CO + NO reaction over Pd(111) and Pd(100). J Vac Sci Technol A-Vac Surf Films 13(3):1539–1543
20. Tao F, Grass ME, Zhang YW, Butcher DR, Renzas JR, Liu Z, Chung JY, Mun BS, Salmeron M, Somorjai GA (2008) Reaction-driven restructuring of Rh–Pd and Pt–Pd core-shell nanoparticles. Science 322(5903):932–934
21. Araya P, Diaz V (1997) Synergism in the reaction of CO with O_2 on bimetallic Rh–Pd catalysts supported on silica. J Chem Soc-Faraday Transctions 93(21):3887–3891
22. Araya P, Diaz V, Cortes J (1998) Reducibility of bimetallic Pd–Rh catalysts and its relation with synergism in the oxidation reaction of CO with O_2. J Chem Res (4):194–195
23. Basile F, Fornasari G, Trifirò F, Vaccari A (2002) Rh–Ni synergy in the catalytic partial oxidation of methane: surface phenomena and catalyst stability. Catalysis Today 77(3): 215–223
24. Oh SH, Carpenter JE (1986) Platinum rhodium synergism in 3-way automotive catalysts. J Catal 98(1):178–190
25. Yoon KJ, Kang HK, Yie JE (1997) Synergism and kinetics in CO oxidation over palladium–rhodium bimetallic catalysts. Korean J Chem Eng 14(5):399–406
26. Araya P, Berrios JP, Wolf EE (1992) Activity and infrared studies during carbon monoxide oxidation over bimetallic palladium–rhodium/silica catalysts. Appl Catal A: Gen 92(1):17–27

27. Araya P, Weissmann C (2000) FTIR study of the oxidation reaction of CO with O_2 over bimetallic Pd–Rh/SiO_2 catalysts in an oxidized state. Catal Lett 68(1–2):33–39
28. Mergler YJ, Ramsaransing DRG, Nieuwenhuys BE (1994) An infrared spectroscopic study of co and no adsorption on bimetallic Pd–Rh/SiO_2 catalysts. Recueil Des Travaux Chimiques Des Pays-Bas-J R Neth Chem Soc 113(10):431–438
29. Araya P, Ferrada C, Cortes J (1995) Activity during reduction of no by co over bimetallic palladium rhodium/silica catalysts. Catal Lett 35(1–2):175–181
30. Tao F, Grass ME, Zhang YW, Butcher DR, Aksoy F, Aloni S, Altoe V, Alayoglu S, Renzas JR, Tsung CK, Zhu ZW, Liu Z, Salmeron M, Somorjai GA (2010) Evolution of structure and chemistry of bimetallic nanoparticle catalysts under reaction conditions. J Am Chem Soc 132(25):8697–8703
31. Tao F, Grass M, Zhang Y, Butcher DR, Aloni S, Tsung CK, Liu Z, Altoe V, Renzas JR, Aksoy F, Mun BS, Salmeron M, Somorjai G (In preparation, 2010)
32. Oh SH, Fisher GB, Carpenter JE, Goodman DW (1986) Comparative kinetic-studies of CO–O_2 and CO–NO reactions over single-crystal and supported rhodium catalysts. J Catal 100(2): 360–376
33. Cortes J, Valencia E (2004) Monte Carlo studies (MCLH simulations) of the CO–NO reaction on disordered substrates and their relation with experiments. J Phys Chem B 108(9):2979–2986
34. Muraki H, Shinjoh H, Fujitani Y (1986) Reduction of no by co over alumina-supported palladium catalyst. Ind Eng Chem Prod Res Dev 25(3):419–424
35. Loffreda D, Simon D, Sautet P (1998) Molecular and dissociative chemisorption of NO on palladium and rhodium (100) and (111) surfaces: a density-functional periodic study. J Chem Phys 108(15): 6447–6457
36. Vesecky SM, Rainer DR, Goodman DW (1996) Basis for the structure sensitivity of the CO + NO reaction on palladium. J Vac Sci Technol A 14(3):1457–1463
37. Zaera F, Sales JL, Gargiulo MV, Ciacera M, Zgrablich G (2007) On the formation of nitrogen islands on rhodium surfaces. J Phys Chem C 111(21):7795–7800
38. Zaera F, Gopinath CS (2002) Effect of coverage and temperature on the kinetics of nitrogen desorption from Rh(111) surfaces. J Chem Phys 116(3):1128–1136
39. Chuang SSC, Tan CD (1998) Mechanistic studies of the NO–CO reaction on Rh/Al_2O_3 under net-oxidizing conditions. J Catal 173(1):95–104
40. Gustafson J, Westerstrom R, Resta A, Mikkelsen A, Andersen JN, Balmes O, Torrelles X, Schmid M, Varga P, Hammer B, Kresse G, Baddeley CJ, Lundgren E (2009) Structure and catalytic reactivity of Rh oxides. Catal Today 145:227–235